

Assessment and Categorization of TLE Orbit Errors for the US SSN Catalogue

Tim Flohrer

Aboa Space Research Oy (ASRO) at Space Debris Office, ESA/ESOC, Darmstadt, Germany

Tim.Flohrer@esa.int

Holger Krag

Space Debris Office, ESA/ESOC, Darmstadt, Germany

Heiner Klinkrad

Space Debris Office, ESA/ESOC, Darmstadt, Germany

Abstract

The Space Debris Office at ESA predicts conjunction events based on Two-Line Element (TLE) data obtained from the US Space Surveillance Network. Currently two ESA missions, the Low-Earth orbiting satellites ERS-2 and Envisat, are covered. For all conjunction events that passed a so-called smart sieve filtering the related collision risk is assessed and provided in a bulletin that is distributed by email daily. In case a high-risk conjunction event is forecast external tracking data of the chaser are acquired. Orbit determination using these data gives improved state and covariance information of the chaser. A subsequent re-assessment of the collision risk allows to decide on the necessity of collision avoidance maneuvers and to support the planning of necessary maneuvers.

At ESA's Space Debris Office the central tools for analyzing conjunction events are the collision risk assessment software CRASS and the orbit determination software ODIN. The risk assessment faces the problem that no covariance information is available for the TLE data set. CRASS copes with this issue by introducing pre-defined look-up tables for the initial covariance that are sorted by eccentricity, perigee height, and inclination. Through ODIN the covariance information is obtained from comparing states derived directly from the TLE data with states resulting from an orbit determination using pseudo-observations derived from TLE data. The obtained covariance information reflects the limitations of the TLE (SGP4) orbit model combined with the limitations of ODIN in terms of orbit determination and propagation accuracy. Until now the CRASS look-up table contains only a limited number of orbit classes.

Recently, a new command-line version of ODIN has been developed, allowing repetitive, fully automated analyses. Thus, the application of the covariance estimation procedure to the entire TLE catalogue becomes feasible. We address the orbit determination and propagation quality of ODIN by comparing orbits determined from precise radar tracking with external high-precision orbits obtained from laser-tracking and Doppler ranging, and by comparing propagated states to these high-precision orbits. For a current catalogue we assess the TLE orbit errors in along-track, cross-track, and out-of-plane coordinates (i.e. as function of eccentricity, inclination and perigee height). This analysis provides a more realistic look-up table for the collision risk assessment with CRASS. Insights into the applicability of the TLE theory to certain classes of orbits will be helpful in particular for the selection of data product formats for the European Space Situational Awareness system that is under study. Finally the presented approach may be the basis for comparisons of snapshots of the TLE catalogue of past epochs.

1. INTRODUCTION

Routinely, the Space Debris Office at ESA predicts conjunction events for currently two ESA missions, the Low-Earth orbiting satellites ERS-2 and Envisat. The orbits for potential chaser objects are taken from Two-Line element (TLE) data obtained from the US Space Surveillance Network. For all conjunction events that passed a so-called smart sieve filtering the related collision risk is assessed and provided in a bulletin that is distributed via email daily. ESA uses the tool CRASS (Collision Risk Assessment Software, [6]) to identify conjunction events and to estimate the associated collision risk [3, 8, 11, 9]. The risk of collisions in orbit is not hypothetical; three accidental collision events involving objects of the TLE catalog have been identified so far [12].

The prediction of conjunction events is only possible if the orbits of potential chaser objects are known. The orbit determination of these objects requires regular tracking by ground-based or space-based sensors. Moreover the collision risk for objects not accessible by the tracking sensors - typically these are small-sized objects - can only be estimated using statistical flux data. For some representative orbits the mean time between a collision with objects of diameters $d > 1$ mm, $d > 1$ cm, and $d > 1$ dm is listed in [11].

In case a high-risk conjunction event is forecast based on TLE data the operators of the spacecraft supported by the Space Debris Office decide whether dedicated tracking data of the chaser should be acquired. Orbit determination using these tracking data gives improved state and covariance information of the chaser. A subsequent re-assessment of the collision risk with CRASS considering this updated information allows to decide on the necessity of collision avoidance maneuvers and to support the planning of necessary maneuvers. Radar observations of chasers usually are acquired by the German radar TIRA (Tracking and Imaging Radar) located at Wachtberg, Germany, which is operated by FGAN (Research Establishment for Applied Sciences), or they may be acquired using Armor radar units on the vessel Monge that is operated by the French Ministry of Defense [4]. These observations can be carried out on very short notice and the observational data are immediately forwarded to the Space Debris Office. There, observed ranges, range rates, azimuth and elevation angles are used in an orbit determination process with the tool ODIN (Orbit Determination with Improved Normal Equations) [7]. A-priori information for the orbit, and additional information used in the orbit determination are extracted from ESA's DISCOS database. The overall process of observation data conversion, a-priori orbit generation, and orbit determination has been widely automated recently [9]. The different development stages of ESA's process applied to high-risk conjunction events can be traced in [8, 9, 10, 11].

The risk assessment faces the problem that no covariance information is available for the TLE data set. CRASS copes with this issue by introducing pre-defined look-up tables for the initial covariance that are sorted by eccentricity, perigee height and inclination. This information is applied to the propagation of the state and covariance information of identified chasers. Those look-up tables are clearly a central parameter in CRASS. But until now the CRASS look-up table contains only a limited number of exemplary orbit classes. As it is envisaged to keep the use of external tracking facilities at a minimum, the optimization and improvement of the look-up tables was selected for a detailed study.

2. APPLIED METHODOLOGY

The covariance look-up tables that are used in CRASS were generated through ODIN by comparing states derived directly from the TLE data to states resulting from an orbit determination using pseudo-observations followed by a numerical propagation. Those pseudo-observations were derived from the TLE data and were generated by ODIN. Fig. 1 outlines this applied methodology. Finally, the desired covariance information is obtained from the statistical analysis of the residuals in the UVW -space (radial, along-track, out-of-plane).

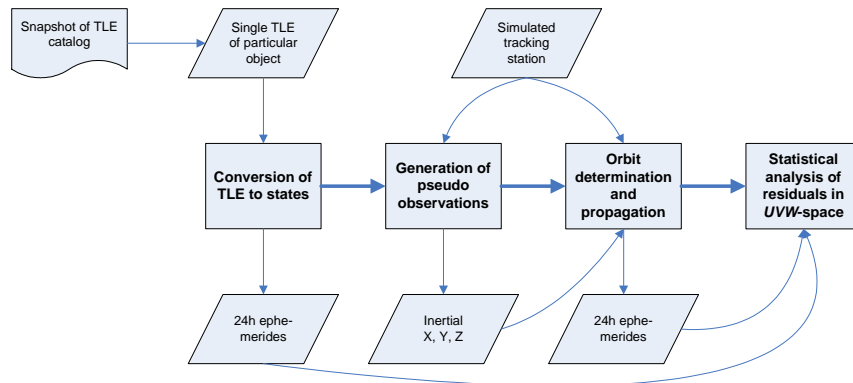


Fig. 1. Outline of the used methodology for TLE accuracy assessment

Using this methodology the obtained covariance information reflects the limitations of the TLE (SGP4) orbit model of the chosen object combined with limitations of the tool ODIN in terms of orbit determination and orbit propagation accuracy, and of course any errors introduced in the generation of the pseudo observations. If ODIN's orbit determination and propagation accuracy, and the accuracy of the pseudo observations are known, the described methodology leads to a qualitative description of the limitation of the TLE (SGP4) orbit model. The chosen approach gives, however, only an assessment of the internal model truncation error of the used TLE theory. In particular the problem of overlap differences between pseudo-observations generated from subsequent TLE-sets is not touched, as for each object only one single 24-hour arc is considered in the analysis. With this approach it is further not possible to discriminate between intrinsic errors in the SGP4-theory or biases that affect the TLE orbit model in principle, and errors introduced during the TLE generation.

The described approach is not new. The currently used covariance look-up tables in CRASS were set up during the CRASS development by manually processing selected objects, which were considered being exemplary [7]. Fourteen objects, each representing one class in the space "inclination - eccentricity - perigee height" were used [6]. In addition the identical approach was applied to study a sample of 21 objects with a perigee height below 450 km [11]. The authors stress that a major benefit from this approach is saving computation time during CRASS runs, as the estimated covariance values remain fixed in the generated look-up-table.

A new command-line add-on to the ODIN software has been developed recently that allows repetitive, fully automated analyses [9]. With this tool the application of the described covariance estimation procedure to the entire TLE catalogue became feasible. We use a similar parameterization of the experiment as [11]: for each object in the catalog an orbit spanning 24 hours, centered on the TLE-epoch is generated using the SGP4 theory. Pseudo-observations (Cartesian states in the inertial frame) are generated accordingly. In the orbit determination and for the numerical propagation of the determined states over the 24 hours arc the MSIS-90 atmospheric model, luni-solar perturbations, radiation pressure, and the Earth's gravity field modeled up to degree and order 30 (JGM3) are considered. Area and mass of the satellite were taken from the DISCOS database. If those values were not available default values of 10 kg and 1 m² are used.

According to this procedure for each object in the TLE catalog two orbits with a step size of 30 seconds are generated with ODIN. Both orbits are compared in the UVW -space. The transformation of the orbital states follows the outline in [10]. The TLE-based states \mathbf{x}_{TLE} and the numerically propagated states \mathbf{x}_{num} are both transferred into the UVW -space that is defined from \mathbf{x}_{TLE} using the transformation matrix \mathbf{R} :

$$\mathbf{R} = \begin{pmatrix} U_x & U_y & U_z \\ V_x & V_y & V_z \\ W_x & W_y & W_z \end{pmatrix} ; \quad \mathbf{U} = \frac{\mathbf{x}}{\|\dot{\mathbf{x}}\|} \quad \mathbf{W} = \frac{\mathbf{x} \times \dot{\mathbf{x}}}{\|\mathbf{x} \times \dot{\mathbf{x}}\|} \quad \mathbf{V} = \mathbf{W} \times \mathbf{U} ,$$

We calculate the standard deviation of the residuals between the transformed states \mathbf{x}'_{TLE} and \mathbf{x}'_{num} in U , V , and W direction. The obtained standard deviations σ_{AU} , σ_{AV} , and σ_{AW} give the desired estimates for the TLE uncertainties as input for the covariance look-up tables.

There are (at least) the following alternative ways to determine the covariance data:

- TLE uncertainties are estimated frequently from the differences in the overlapping arcs spanned by subsequent TLEs (this method is applied in the routine conjunction analyses and collision risk estimates at CNES [13]). In this method each TLE of a consecutive pair is propagated correspondingly forward and backward to the epoch of the other one and the states at those epochs are compared. This method tests, however, the consistency between subsequent TLE-sets only. Even if we assume unbiased measurements and error-free orbit determination and TLE generation, successive TLE's might be correlated due to theory errors. Such errors cannot be detected with this method.
- With knowledge (or at least with reasonable assumptions) on the TLE production process, in particular on the acquiring sensor and the data acquisition epochs, the measurement errors and potentially biases of those sensor may be estimated from reconstructing the raw observations. This step should be considered as an additional step to our presented method.

- The optimal approach is to assess the covariance information from comparing TLE-based orbits to operational orbits obtained from satellite operators, or from comparison to high-accuracy post-processing orbits, as they are available for some satellites to the scientific community from coordinated services (such as the IGS, ILRS, IDS, etc.). This approach is only possible for a limited number of satellites and may thus not cover all orbit regions (or potential chasers) appropriately. It is nevertheless an important and preferred verification of all other methods.

See [11] for a comparison of our numerical fit approach with the subsequent-TLE approach. This comparison concludes to use the numerical fit method, as it is closer to the mean value of states obtained from operational orbits.

3. VERIFICATION OF ORBIT DETERMINATION ACCURACY WITH ODIN

In the presented method we neglect errors introduced by the orbit determination and propagation. An assessment of the orbit determination and propagation accuracy using our tool ODIN is thus required. This can be achieved by comparing orbits obtained from precise radar tracking with high-precision orbits obtained from laser-tracking and Doppler ranging (DORIS), and by comparing propagated states with the high-precision orbits. The generation of pseudo observations cannot be assessed independently as the same software code as in the orbit determination is used.

We used high-precision orbits of Envisat determined by ESOC that are based on DORIS and SLR tracking data. The orbit accuracy was found to be around 10 cm, with the radial orbit accuracy of 3 cm [1, 2] from the orbit comparison campaign conducted by ESOC in 2003. Precise radar tracking of Envisat was acquired by FGAN on June 6 and 7 2006. Three tracks were acquired in total (starting at 11:33 on June 6, 09:02 and 10:41 on June 7). Observed ranges, azimuth and elevation data were used in the orbit determination with ODIN. Using a-priori information from a current TLE data set the orbit determination revealed a RMS of the accepted measurements in range of 17 m, in azimuth of 0.004 deg, and in elevation of 0.008 deg. The determined orbit was then propagated using ODIN's propagation module and assuming a not fitted ballistic coefficient of 2.2 as starting point.

The quality of the propagation routine was assessed by propagating a single state of the high-precision orbit over the analysis period from 2006-Jun-06 00:00 to 2006-Jun-08 00:00. Fig. 2 shows the obtained propagation quality. The largest deviations within 24 hours stay below 40m, nearly entirely in along-track direction. The standard deviation of the residuals over 24hours is 1 m in radial, 19 m in along-track and 2 m in out-of-plane direction. Fig. 3 gives the residuals between the orbit obtained from the three observed radar tracks and the high-precision orbit. The standard deviation is found to be 2 m in radial, 4 m in along-track and 14 m in out-of-plane direction. This altogether leads to the conclusion that our proposed method is able to assess TLE uncertainties down to the order of about 20 m, if 24 hour arcs around the TLE epoch are used.

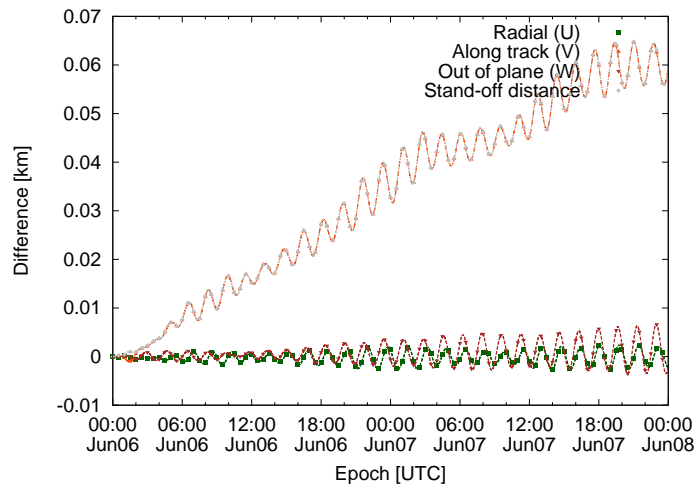


Fig. 2. Comparison of a state propagated with ODIN (unfitted $c_D=2.2$) to an external high-precision (post-processed) orbit determined using SLR and DORIS data.

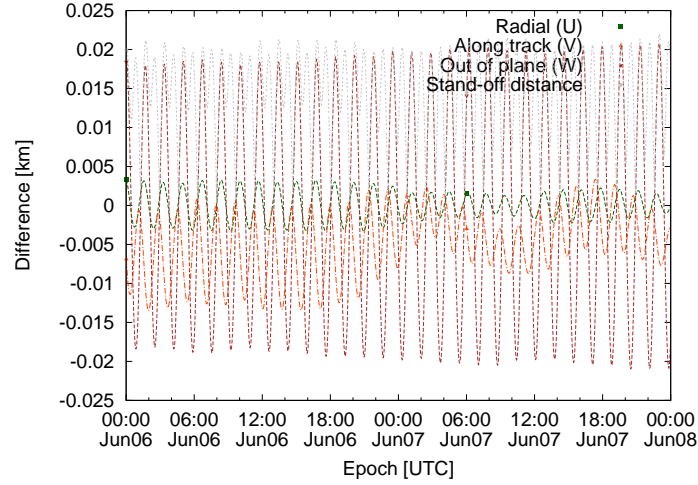


Fig. 3. Comparison of states propagated from an orbit determined from three acquired radar tracks to a external high-precision (post-processed) orbit determined using SLR and DORIS data.

4. RESULTS OF ASSESSMENT PROCESS

In this section we present the estimated TLE orbit uncertainties in radial U , along-track V , and out-of-plane W direction for a current snapshot of the TLE catalogue.

4.1 Overview of used population snapshots

All data was taken from ESA's DISCOS database that contains orbital elements in TLE format together with additional information for Earth-orbiting objects. Source of the TLE sets is the US Space Surveillance Network. A snapshot of the TLE catalogue was generated using the nearest TLE-set to the reference epoch, with cut-offs at 30 days prior and after that epoch.

For the reference epoch 2008-Jan-01 the snapshot of the TLE catalogue consists of 11470 individual objects, of which 11286 were successfully processed.

For further analyses we classify the objects according to their orbits:

- LEO (Low-Earth orbits): Apogee altitude $h_A < 2000$ km
- GEO (Geostationary orbits): Perigee altitude $h_P > 40164$ km and apogee altitude $h_A < 44164$ km
- MEO (Medium-Earth orbits): Perigee altitude $h_P > 2000$ km and apogee altitude $h_A < 40164$ km
- GTO (Geostationary transfer orbits): Perigee altitude $h_P < 2000$ km and apogee altitude $h_A > 40164$ km
- HEO (Highly elliptical orbits): all other objects

Fig. 4 and Fig. 5 give the object classification in the a/e and in the e/i space. We will present our results in a similar coordinate system as in Fig. 5.

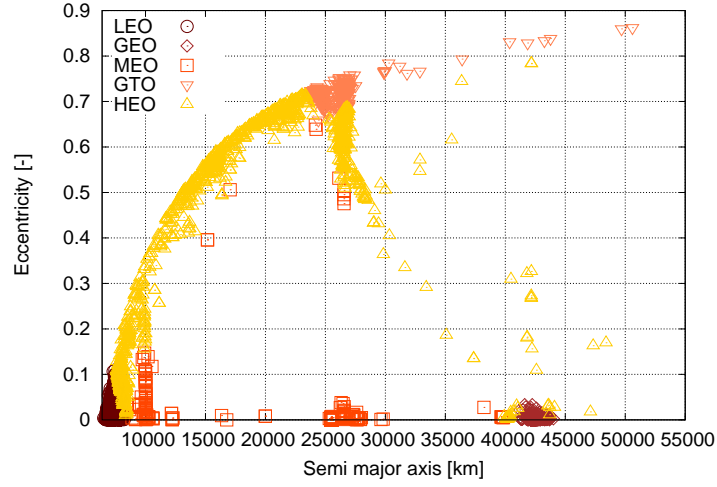


Fig. 4. Reference population of 2008-Jan-01, eccentricity vs. semi major axis.

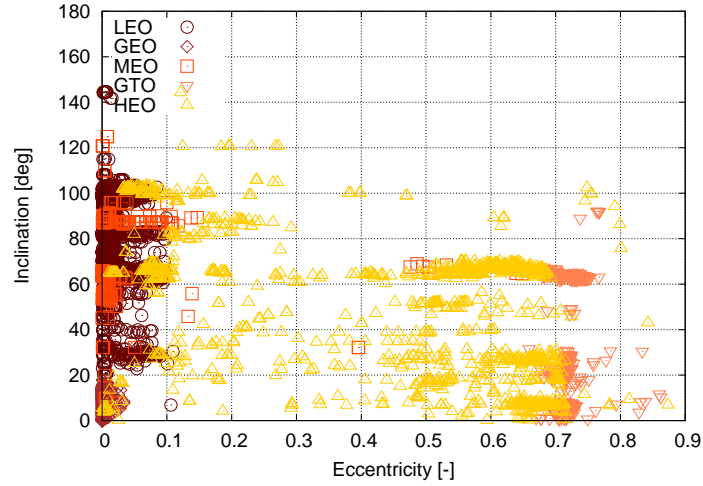


Fig. 5. Reference population of 2008-Jan-01, eccentricity vs. inclination.

4.2 Results for most recent snapshot

The analysis results for the entire snapshot population are shown in (Fig. 6). Standard deviations up to about 5 km are possible in certain regions in the along-track direction. In general, the radial and out-of-plane components show smaller uncertainties than in the along-track direction in all regions. This is an expected result, as the insufficiencies of the drag modeling, as well as any epoch registration errors contained in the observations, will appear in the along-track component most prominently. Further, there are systematic patterns in all three components visible in the plots, in particular as a function of the eccentricity. Objects in low-eccentric orbits seem to be covered better by the TLE-theory than objects in orbits with higher eccentricities. There are also patterns visible that indicate a dependency on the inclination. Leaving the circular orbits out, objects in low-inclined orbits show higher uncertainties in radial and along-track direction compared to objects orbiting in higher inclinations. This is slightly different in the out-of-plane component, where the largest uncertainties are found at medium inclinations, centered on ~ 40 deg. It is difficult to give the reason for the observed pattern, as the applied process for the TLE generation is unknown. A study addressing the found pattern should include the bridging of gaps in the observations, or the performance of the used sensors.

For detailed investigation we have repeated this analysis for each class of orbits: LEO, GEO, MEO, GTO and HEO. Fig. 7 shows that in these regions lowest TLE uncertainties might be expected. With the radial component being described best, the out-of-plane component described similarly well and the along-track component reaching up to 0.7 km in the worst cases, the effect of the radar observations of the LEO region becomes visible.

The MEO region comprises the smallest number of objects in our analysis. Fig. 8 shows that the TLE uncertainties in all components are extremely low for the orbits used for navigational satellites (circular orbits with inclination around 50-60 deg). Other circular orbits in the MEO region are also of low uncertainties, but the eccentric orbits indicate some significant limitations of the SDP theory.

The analysis of the objects classified as belonging to the GTO region (Fig. 9) reveals that two groups of objects might be distinguished. First class are GTOs in low-inclined orbits that have a low uncertainty in the out-of-plane component, but have the largest (even in the global scale) uncertainty in the along-track component and a significant uncertainty of about 2.5 km in the radial component. The second class comprises GTOs in higher inclination orbits. These objects show much lower uncertainties in the radial and along-track component, but a higher uncertainty in the out-of-plane component. This might indicate that these two groups are covered by different sensors (radar and telescopes) and/or that there are other systematic effects in the TLE-generation process that affect most the GTOs in low inclination orbits.

A similar pattern as observed for the GTOs is found in the other highly-elliptical orbits, in the HEO class (see Fig. 10). Objects orbiting in eccentric, low inclination orbits show large uncertainties in the radial and along-track component, while having moderate uncertainties in the out-of-plane component. From all objects in eccentric orbits those orbiting in the inclination band between 60 and 65 deg are of significantly lower uncertainty, in particular in the radial and along-track component. Fig. 10 also nicely supports the general statement that circular orbits show lower uncertainties than eccentric orbits.

The GEO class is analyzed in a slightly different domain, in the RAAN (right ascension of the ascending node) vs. inclination space, as for objects in the GEO class the eccentricity is always low. Typically, both, uncertainties in the along-track and in the radial component, are better than 0.5 km (see Fig. 11). Of much lower uncertainty is the radial component that is found better than 0.1 km. From the plot (especially looking at the radial component) we may also suspect that in the TLE generation process active (e.g. maneuvering) objects are associated with a higher uncertainty in all components. In GEO only those active objects might be kept at 0 deg inclination at any RAAN angle, which is nicely shown in (Fig. 11).

We have combined all described class-wise analyses in Tab. 1. This table gives the average values for the three analyzed components. All results for a certain class of objects were filtered for outliers using a 6-sigma criterion. Further, the number of total and used (i.e. non-rejected) objects is given.

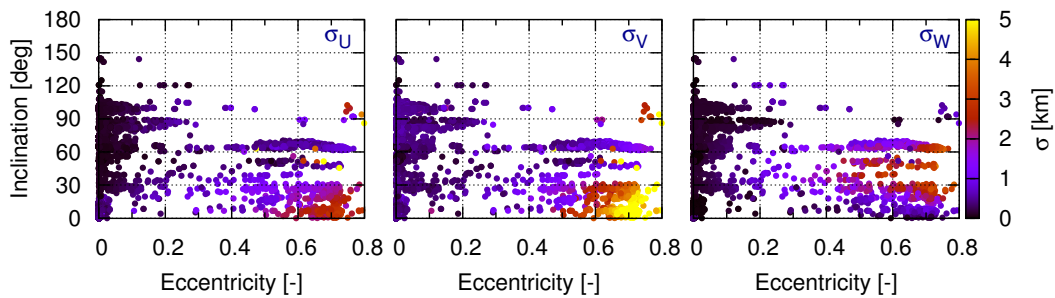


Fig. 6. Estimated uncertainties of all objects in the snapshot of the TLE catalog of 2008-Jan-01 in radial (U), along-track (V) and out-of-plane (W) direction, displayed as function of eccentricity and inclination at the analysis epoch.

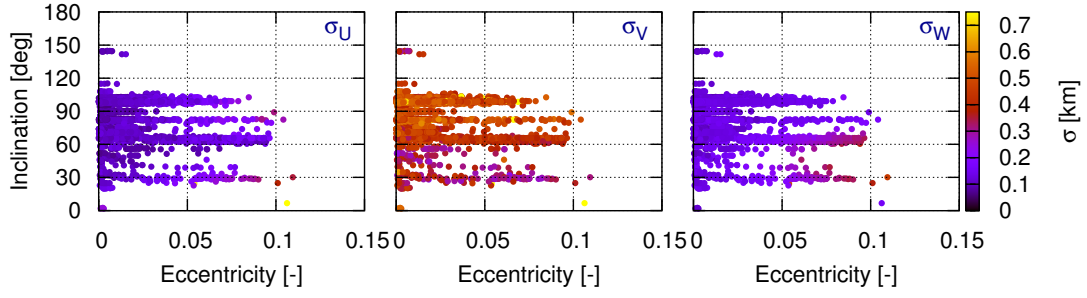


Fig. 7. Estimated uncertainties of all objects in the LEO class of the snapshot of the TLE catalog of 2008-Jan-01 in radial (U), along-track (V) and out-of-plane (W) direction, displayed as function of eccentricity and inclination at the analysis epoch.

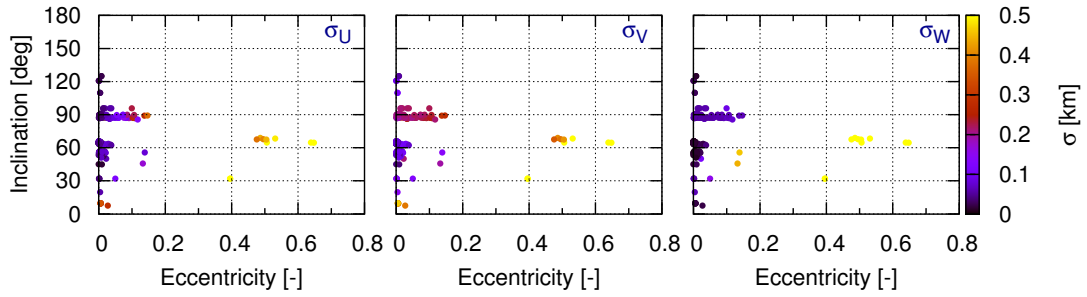


Fig. 8. Estimated uncertainties of all objects in the MEO class of the snapshot of the TLE catalog of 2008-Jan-01 in radial (U), along-track (V) and out-of-plane (W) direction, displayed as function of eccentricity and inclination at the analysis epoch.

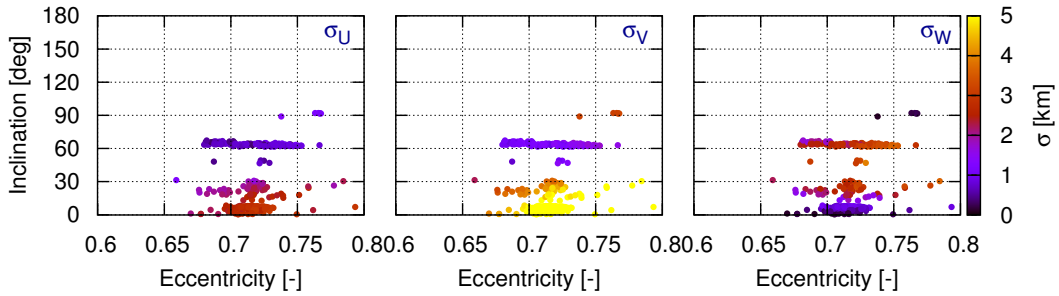


Fig. 9. Estimated uncertainties of all objects in the GTO class of the snapshot of the TLE catalog of 2008-Jan-01 in radial (U), along-track (V) and out-of-plane (W) direction, displayed as function of eccentricity and inclination at the analysis epoch.

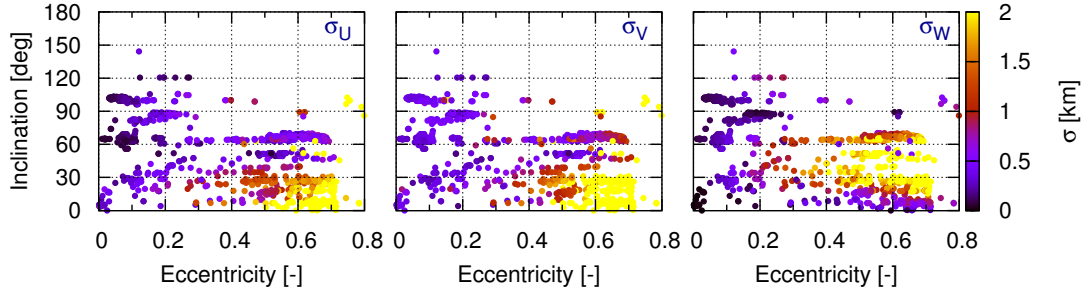


Fig. 10. Estimated uncertainties of all objects in the HEO class of the snapshot of the TLE catalog of 2008-Jan-01 in radial (U), along-track (V) and out-of-plane (W) direction, displayed as function of eccentricity and inclination at the analysis epoch.

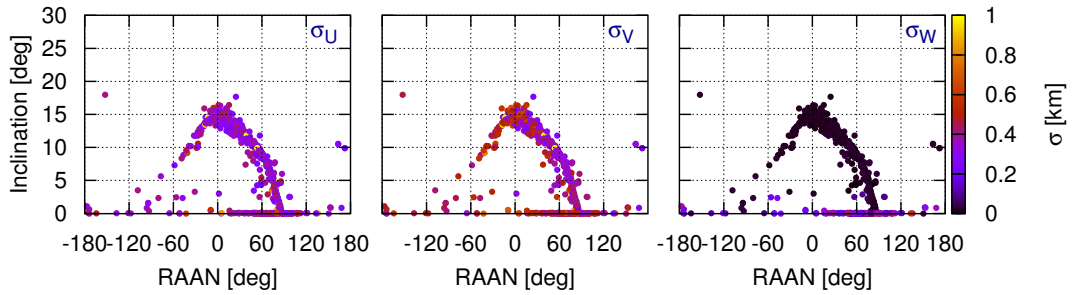


Fig. 11. Estimated uncertainties of all objects in the GEO class of the snapshot of the TLE catalog of 2008-Jan-01 in radial (U), along-track (V) and out-of-plane (W) direction, displayed as function of right ascension of the ascending node and inclination at the analysis epoch.

Table 1: Tabulated results of the analysis of the TLE catalog of the epoch 2008-Jan-01 (the ratio “used number of objects vs. total number of objects” refers to a 6-sigma filtering for outliers).

Orbit regime	Number of objects (used/total)	Averaged σ_U [km]	Averaged σ_V [km]	Averaged σ_W [km]
LEO	8454/8463	0.102	0.471	0.126
MEO	317/321	0.073	0.131	0.054
GTO	371/371	1.960	3.897	1.808
HEO	1237/1245	0.824	1.367	1.059
GEO	878/886	0.359	0.432	0.086

A comparison of the obtained results with the results presented in [6] reveals that there is a good match for low circular orbits with inclinations higher than 30 deg (see Tab. 2). This is the region of particular concern for ERS-2 and Envisat conjunction analysis, as most potential chasers orbit in these regions. There is, however, a significant mismatch for the non-circular orbits and the orbits with perigee altitudes above 800 km. The covariance values set in the CRASS look-up table tend to be pessimistic in most cases. The general trend and the relative ratios between the analyzed classes match quite well.

Table 2: Look-up table [m] of averaged results from the analysis of the catalog snapshot of 2008-Jan-01

$e < 0.1$		$i < 30 \text{ deg}$	$30 \text{ deg} < i < 60 \text{ deg}$	$i > 60 \text{ deg}$
$h_P < 800 \text{ km}$	RAD (U)	67	107	115
	A-T (V)	118	308	517
	C-T (W)	75	169	137
$800 \text{ km} < h_P < 25000 \text{ km}$	RAD (U)	191	71	91
	A-T (V)	256	228	428
	C-T (W)	203	95	114
$h_P > 25000 \text{ km}$	RAD (U)	357	-	-
	A-T (V)	432		
	C-T (W)	83		
$e > 0.1$		$i < 30 \text{ deg}$	$30 \text{ deg} < i < 60 \text{ deg}$	$i > 60 \text{ deg}$
$h_P < 800 \text{ km}$	RAD (U)	2252	629	494
	A-T (V)	4270	909	814
	C-T (W)	1421	2057	1337
$800 \text{ km} < h_P < 25000 \text{ km}$	RAD (U)	1748	1832	529
	A-T (V)	3119	1878	817
	C-T (W)	971	1454	1570
$h_P > 25000 \text{ km}$	RAD (U)	402	4712	-
	A-T (V)	418	6223	
	C-T (W)	83	1208	

Comparing the results with the fitted polynomial in [11], where the analysis was limited to objects with the perigee below 450 km reveals a good match. The residuals between the polynomial and our estimation are for U , V , and W in the 10 m to 50 m range, except for objects in low inclination, highly eccentric orbits. In these particular cases the residuals may reach up to 3 km. This might indicate a problem with one single object that was selected to present the region around 7 deg inclination, 0.7 eccentricity.

4.3 Comparison with historical snapshots

As our analysis environment allows fully automated runs with ODIN, it is easy to compare the result to other population snapshots, i. e. to TLE catalogs of past epochs. We performed seven additional analyses for which we used DISCOS data covering all objects in the catalog with a TLE-epoch of ± 30 days around 1990-Jul-01, 1993-Jan-01, 1995-Jul-01, 1998-Jan-01, 2000-Jul-01, 2003-Jan-01, and 2005-Jul-01.

Fig. 12 gives the history of the averaged standard deviation per class and component. The assigned error bars denote the standard deviation of the averaged value resulting from the averaging process. Fig. 12 shows that in the GEO region along-track and radial component were worse by a factor of ~ 1.5 between 1995 and 2003, but are steadily improving since 2003. The out-of-plane component is not affected. The reason for this signal is unclear. The LEO and MEO classes show no changes over time. The apparent drifts and variations over time in the GTO regime will need further investigations to rule out effects stemming from the two different uncertainty classes of objects that are found in these regions.

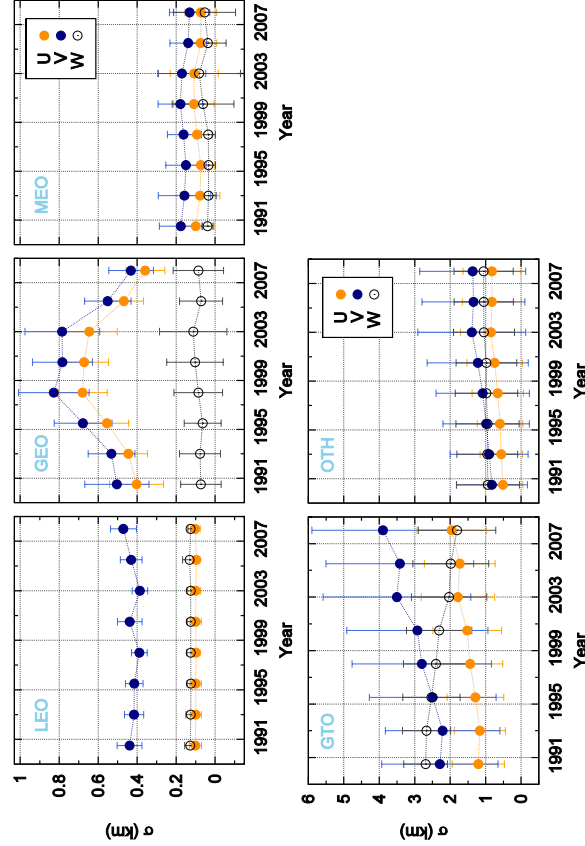


Fig. 12. Evolution of the estimated uncertainties of all objects, grouped in their classes, in radial (U), along-track (V) and out-of-plane (W) direction, displayed as function of the analyzed epoch.

5. CONCLUSION

We have analyzed intrinsic TLE uncertainties for the entire snapshot of a current TLE catalog. In radial/along-track/out-of-plane direction the applied analysis method compared the states derived directly from the TLE data with states resulting from an orbit determination using pseudo-observations followed by a numerical propagation. We have shown, by comparing with a post-processed highly accurate orbit of Envisat, that our used tool ODIN is able to meet the required orbit determination and orbit propagation accuracies.

Our results make it possible to classify intrinsic TLE uncertainties. It is proposed to keep this classification in the domain eccentricity-inclination-perigee height, as it is implemented in ESA's collision avoidance process with the central tool CRASS. We found that the estimated uncertainties show in some regions larger differences to the values used in CRASS, which stresses the need for setting narrower classes in CRASS' covariance look-up-tables. The idea of having one entry per object in the covariance look-up-table needs further study, as well as possible daily re-analysis for those objects involved in conjunction events.

A comparison of the results from an analysis of historical TLE catalog snapshots showed a good consistency of the estimated uncertainties over the last 18 years, except for the GEO region, where a degraded uncertainty over a few years has been observed. As expected, TLE uncertainties are higher for elliptical orbits.

Future work after this study will be to introduce the obtained results into CRASS. In principle it needs to be investigated whether objects of similar orbits should be combined in the covariance look-up tables. The alternative would be to have each individual object listed in the look-up table. New objects for which the estimation of the covariance information has not yet been carried out would be covered based on interpolating the data of neighboring orbit classes. It is intended to keep the classification of the covariance in the inclination-eccentricity-perigee height space (as proposed in [11]).

Insights into the applicability of the TLE theory to certain classes of orbits, in particular as function of individual sensor performance and observation scenarios will be helpful for the selection of data product formats for the European Space Situational Awareness system that is under study. The results further underline that the availability of reliable and up-to-date covariance information is essential for providing SSA-related products, including services dealing with threats imposed by conjunction events. One well known example is that not performing collision avoidance maneuvers by having better covariance information available might extend the operational time of a mission and helps meeting space debris mitigation goals.

6. REFERENCES

- 1 Otten M. and Boonkamp H., Estimation of the Absolute Orbit Accuracy of Envisat, European Space Operation Centre, Darmstadt, May 2003, available from nng.esoc.esa.de/envisat/results/campaign.pdf
- 2 Zandbergen, R., M. Otten, P. L. Righetti, D. Kuijper, and J. M. Dow, Routine Operational and High-precision Orbit Determination of Envisat, *Adv. Space Res.*, Vol. 31, No. 8, pp. 1953-1958, 2008.
- 3 Klinkrad, H., J. Alarcón, N. Sanchez, Operational Collision Avoidance with Regard to Catalog Objects, in: H. Klinkrad, *Space Debris: Models and Risk Analysis*, Springer, Berlin, Heidelberg, New York, 2006.
- 4 Klinkrad, H., The Current Space Debris Environment and its Sources, in: H. Klinkrad, *Space Debris: Models and Risk Analysis*, Springer, Berlin, Heidelberg, New York, 2006.
- 5 Alarcón-Rodríguez, J., F. M. Martínez-Fadrique, H. Klinkrad, A. Rudolph, and F. Bosquillon de Frescheville, Conjunction Event Predictions for Operational ESA Satellites, Eighth International Conference on Space Operations, May 17-21 2004, Montréal, Canada.
- 6 Alarcon, J. R., Development of a Collision Risk Assessment Tool, Final Report, ESA contract 14801/00/D/HK, GMV S. A., 2002.
- 7 Alarcón, J. R. and Klinkrad, H. and Cuesta, J. and Martinez, F. M., Independent Orbit Determination for Collision Avoidance, ESA Special Publication SP-587, pp. 331, 2005.
- 8 Alarcon-Rodríguez, J. R., F. M. Martínez-Fadrique, H. Klinkrad, Development of a collision risk assessment tool, *Adv. Space Res.*, Vol. 34, No. 5, pp. 1120-1124, 2004.
- 9 Flohrer T., Krag, H. and Klinkrad H., ESA's Process for the Identification and Assessment of High-risk Conjunction Events, paper presented at the 37th COSPAR Scientific Conference, July 13-20 2008, Montreal, Canada, 2008 (in prep).
- 10 Klinkrad, H. and Alarcon, J. R. and Sanchez, N., Collision Avoidance for Operational ESA Satellites, ESA Special Publication SP-587, pp. 509, 2005.
- 11 Krag, H., H. Klinkrad, and J. R. Alarcón-Rodríguez, Assessment of Orbit Uncertainties for Collision Risk Predictions at ESA, Second IAASS conference "Space safety in a global world", 14 – 16 May 2007, Chicago, USA, 2007.
- 12 Johnson, N. L., Stansbery, E., Whitlock, D. O. , Abercromby K. J., and Shoots, D. History of on-orbit satellite fragmentations. Technical Memorandum NASA/TM2008214779, NASA, 2008.
- 13 Laporte, F. and E. Sasot, Operational Management of Collision Risks for LEO satellites at CNES, AIAA 2008-3409, paper presented at the Space-Ops conference 12-16 May 2008, Heidelberg, 2008.